Received 12 August 2023, accepted 2 September 2023, date of publication 8 September 2023,
date of current version 13 September 2023.

Digital Object Identifier 10.1109/ACCESS.2023.3313504

RESEARCH ARTICLE

Time-Variant Reliability Optimization for Stress Balance in Press-Pack Insulated Gate Bipolar Transistors

HANGYANG LI, TONGGUANG YANG, XINGLIN LIU, (Graduate Student Member, IEEE), JINGYI ZHONG, JIAXIN MO, (Graduate Student Member, IEEE), HAN ZHOU, AND ZHONGKUN XIAO, (Graduate Student Member, IEEE)

Hunan Provincial Key Laboratory of Energy Monitoring and Edge Computing for Smart City, Hunan City University, Yiyang 413000, China

Corresponding author: Hangyang Li (lihangyang_cn@163.com)

This work was supported in part by the Natural Science Foundation of Hunan Province of China under Grant 2023JJ50343, and in part by the Educational Commission of Hunan Province of China under Grant 21A0503 and Grant 21C0662.

ABSTRACT Stress imbalance significantly affects the performance of a press-pack insulated gate bipolar transistor (IGBT). Time-variant loads and conditions lead to the stress fluctuations, exacerbating the impacts. The conventional reliability optimization faces efficiency barriers due to the nested time-variant reliability analysis and design optimization. In this paper, a time-variant reliability optimization approach for press-pack IGBTs is proposed to address the efficiency issue of the IGBT reliability optimization. The performance functions of the maximum and typical stresses are formulated as the optimization objective and constraint. A time-variant reliability optimization model is formulated considering the stress balance reliability degradation within the service cycle. A decoupling algorithm is proposed to transform the nested optimization into a sequential iteration of static reliability optimization and time-variant reliability analysis. The reliability analysis utilizes the performance function continuity in the time domain to reduce the evaluations for the most likelihood points, thereby enhancing efficiency. Numerical and experimental results on an actual IGBT demonstrate the accuracy of the stress balance performance analysis. The time-variant reliability optimization based on the performance functions improves the stress balance performance by 16.3% and meets the reliability requirements within the service cycle. Compared with the conventional double-loop approach, the difference between the solution of the proposed approach with the reference solution is 0.4%, and the efficiency is 334 times that of the double-loop approach. The performance advantages in accuracy and efficiency exhibit the application potential of this approach.

INDEX TERMS Decoupling algorithm, insulated gate bipolar transistor, stress balance, time-variant reliability optimization.

NOMENCLATURE

R	Performance reliability
f	Objective function
g	Constraint function
g_j	j-th Constraint function
X	Design vector
X_i	i-th Design parameter
P	Uncertain vector
$P_l(t)$	l-th stochastic process
$\rho_l(\tau)$	auto-correlation of $P_l(t)$
μ	Mean vector
β	Reliability index
Φ	Cumulative distribution function
E	Expectation operator
S_U	Maximum chip stress
S_T	Typical chip stress
L_0	Chip side length

The associate editor coordinating the review of this manuscript and approving it for publication was Gab-Su Seo.

E_0	Material elastic modulus
N_F	Simulation evaluation
T_F	Time for FEM simulation
t_0	Start of the service cycle
t_f	End of the service cycle
t_i	i-th period unit
m	Number of period unit
ρ_j	Correlation coefficient matrix of g_j
P^M	Most likelihood point
L_j	Linear approximation to j-th constraint function
σ	Standard deviation operation
ε	Convergence limit
c	Safety factor
ρ	Auto-correlation function
Superscripts	
L	Lower bound
R	Upper bound
thr	Threshold value
t	Target value
k	Iteration step
Abbreviation	
IGBT	Insulated gate bipolar transistor

I. INTRODUCTION

An insulated gate bipolar transistor (IGBT) is a fully controlled voltage-driven power semiconductor device. It is widely used in high-voltage and large-capacity power electronics fields, such as traffic traction, industrial frequency converters and flexible direct current transmission [1]. Compared with welded IGBTs, the press-pack IGBT has the advantages of easy series connection, double-sided heat dissipation and high reliability [2]. Therefore, it presents better prospects in high power-density and voltage applications. The clamping force applied to the press-pack IGBT ensures the mechanical and electrical connection between the components and establishes the conductive paths between the heat sink and sources. Excessive pressure may cause the IGBT chips to break. Too little pressure cannot ensure effective thermal contact between components, resulting in thermal failure of the self-heating chips. According to the specification provided by IGBT manufacturers (e.g., ABB, WESTCODE), the external clamping pressure should be controlled at about 12 MPa [3]. The chip self-heating and the component thermal expansion mismatch will lead to the stress imbalance of the IGBT [4]. The contact stress between components determines their electrical/thermal contact states. The performance degradation caused by inappropriate contact stress exacerbates the imbalance [5]. Thus, the stress balance is a crucial factor affecting the electrical/thermal performance of the press-pack IGBT.

Various uncertainties exist in actual engineering, such as manufacturing tolerances, material properties, conditions, and loads. Under the combined influence of the uncertainties, the IGBT performances may fluctuate significantly or even fail [6]. The uncertainties can be divided into two categories [7]. The first is static uncertainty, described as a random variable, such as manufacturing tolerances (e.g., sizes, flatness, roughness) and material properties (e.g., thermal conductivity, modulus of elasticity). The second is time-variant uncertainty, described as a stochastic process consisting of a sequence of time-dependent random variables. For example, in an offshore wind power system, the IGBT clamping force affected by the platform vibration should be considered a stochastic process [8]. In distribution network applications with flexible multi-state switches, the IGBT current load changes with the source/load states, which can be described as a stochastic process [9]. Such time-variant uncertainties lead to varying electrical/thermal stresses on the IGBT components. Excessive stress will cause cumulative damage to the components, significantly reducing the IGBT reliability during the service life [10]. Due to the crucial impact of stress imbalance on performance, it is necessary to explore a time-variant reliability optimization approach for the press-pack IGBT involving stochastic processes.

Reliability optimization can improve structural performance and ensure reliability without eliminating uncertainties [11]. The reliability optimization establishes the links between the uncertain parameters and design options through probability constraints, thereby achieving reliable design solutions. In recent decades, the reliability optimization has become an important research direction in academia and engineering. It has been applied to various fields, such as aerospace [12], automobile [13], electronics [14], [15], pharmacology [16] and civil engineering [17]. Conventional reliability optimization methods only apply to time-invariant systems [18], [19]. To address time-variant reliability problems, Jiang et al. proposed a general solution framework based on time-invariant equivalent strategies [20]. Yu et al. developed a time-variant reliability analysis approach combining the extreme value moment and improved maximum entropy methods for problems with multiple failure modes and temporal parameters [21]. Li et al. explored a direct probability integral method for a ten-story building with tuned mass damper under near-fault stochastic impulsive motions [22]. Wu et al. proposed a time-variant probabilistic feasible region approach using the equivalent inverse most probable point for enhancing efficiency [23]. Objectively speaking, the research on time-variant reliability optimization is still preliminary, and the primary technical bottleneck is efficiency. The solution involves a two-layer nested optimization process. The outer layer optimizes the design variables, and the inner layer performs the time-variant reliability analysis. The time-variant reliability analysis is a challenging issue in the uncertain design field, and its computational burden is much higher than that of static reliability analysis. The nested optimization calls heavily for time-variant reliability analysis involving the time-consuming simulation of IGBT performance. It results in extremely low efficiency.

The literature on the mechanical modeling of IGBT, the time-variant uncertainty measurement of IGBT, and the

TABLE 1. Summary of literature related to this study.

Category	Literature	Support for the contribution of this study
Mechanical modeling of IGBT	[4]Poller et al. 2012; [5]Hasmasan et al. 2014; [2]Deng et al. 2017; [3]Dai et al. 2021; [25]Huang et al. 2021	The literature suggests that stress imbalance within the IGBT significantly affects the electrical performance, and the performance degradation exacerbates the stress imbalance.
Time-variant uncertainty measurement of IGBT	[6]Zhou et al. 2012; [8]Bajrić et al. 2018; [10]Liu et al. 2019; [7]Tian et al. 2022	The literature suggests that the conditions and loads of the IGBT involve time-varying uncertainties, which leads to stress fluctuations and cumulative damage to components.
General time-variant reliability design methods	[20]Jiang et al. 2017; [21]Yu et al. 2018; [22]Li et al. 2022; [18]Xiong and Huang 2022; [23]Wu et al. 2023	The literature proposed the general time-variant reliability design methods, but their application in the IGBT encounters the issue of low efficiency.

general time-variant reliability design methods are summarized in Table 1, forming the motivation for this study. A time-variant reliability optimization approach is proposed to address the reliability optimization modelling and solution for the press-pack IGBT involving stochastic processes. The maximum and typical stress of the chips are considered as performance functions, and time-variant reliability constraints are established to limit the stress balance reliability degradation caused by stochastic processes. The time-variant continuity of the stress response is utilized to reduce the evaluations of time-consuming simulation models. The rest of the paper is organized as follows. Section II explains the influence mechanism of time-variant uncertainties on IGBT stress balance. Section III creates an IGBT time-variant reliability optimization model. Section IV proposes a decoupling algorithm and flowchart. Section V demonstrates the effectiveness of the proposed approach through an actual IGBT application. Section VI concludes.

II. INFLUENCE OF TIME-VARIANT UNCERTAINTIES ON STRESS BALANCE

A. THE STRESS BALANCE ISSUE IN A PRESS-PACK IGBT

A typical press-pack IGBT device is shown in Fig. 1. It contains several sub-modules, divided into two categories: the IGBT sub-module and the fast recovery diode sub-module. In the sub-modules, the components of a silver sheet, bottom molybdenum sheet, chip and top molybdenum sheet are stacked in a plastic housing from bottom to top. The difference is that the IGBT sub-module has a spring pin to connect the chip gate and printed circuit board. The sub-modules are parallel between a collector copper block and emitter copper block. They are clamped into a ceramic package to form an IGBT device. In practice, a clamping force is applied to the upper and lower copper blocks to maintain electrical/thermal contact between components. The silver sheets are used to relieve the stress imbalances between the chips. Liquid cooling conditions are usually set on the top and bottom surfaces of the IGBT device to maintain heat dissipation.

The IGBT stress balance analysis is a multi-physics problem coupled with electricity, thermal and mechanics [24]. The contact pressure between components determines the contact thermal resistance and electrical resistance, as shown in Fig. 2. Thermal resistance and electrical resistance are vital parameters for thermal analysis, affecting the temperature distribution response inside the IGBT. Under the action of

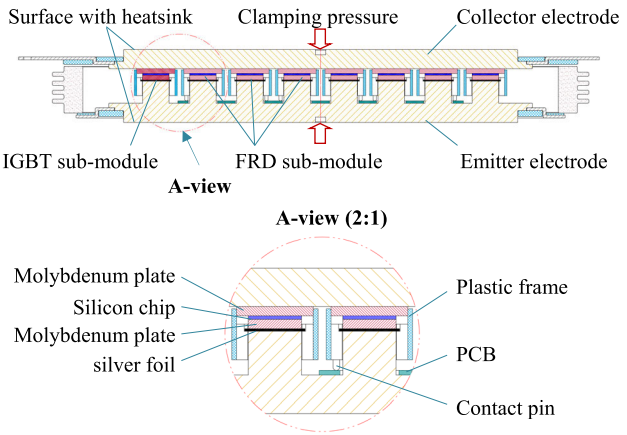

FIGURE 1. A cross-section view of the typical IGBT [25].

non-uniform temperature distribution and mismatched thermal expansion coefficients, the stress imbalance between the chips emerges. Also, the chip heat dissipation is affected by temperature and stress. Therefore, stress balance optimization is the key to improving the IGBT electrical/thermal performance.

B. STRESS BALANCE RELIABILITY DEGRADATION CAUSED BY TIME-VARIANT UNCERTAINTY

For the press-pack IGBT, the function of g characterizes its stress balance performance. $g \geq 0$ indicates that the stress balance meets the requirements. The IGBT contains m-numbers of uncertain parameters, written as $\boldsymbol{P} = (P_1, P_2, \ldots, P_m)$. $\boldsymbol{P}$ causes the performance response of g to be uncertain. The performance reliability is the probability that the stress balance meets requirements under uncertainty, expressed as:

$$R = \Pr\left(g\left(\boldsymbol{X}, \boldsymbol{P}\right) \geq 0\right) \tag{1}$$

where $\boldsymbol{X} = (X_1, X_2, \ldots, X_n)$ is an n-dimensional design vector. Pr represents a probabilistic operation.

Due to time-variant conditions and loads, the IGBT performance response exhibits time-variant characteristics. For example, the chip current changes with the source and load states of the system, and it leads to the time-variant characteristics of the chip heat consumption. For distributed sources of a wind power system, the output power is determined by the wind speed, which is a typical stochastic process [26], [27]. The system load is a dynamic process with statistical laws and

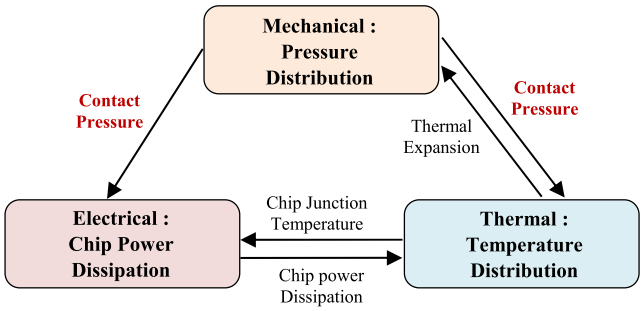

FIGURE 2. The influence mechanism of contact pressure on IGB [25].

random noise, usually described as a stochastic process [28], [29]. Correspondingly, the heat consumption of the chips in the IGBT is a stochastic process.

The time-variant uncertain vector $\boldsymbol{P}$ in Eq. (1) is described as a stochastic process vector: $\boldsymbol{P}(t) = (P_1(t), P_2(t), \ldots, P_n(t))$. A stochastic process is a combination of random variables, which have auto-correlation characteristics in a time domain. $P_l(t)$ denotes the l-th stochastic process of $\boldsymbol{P}(t)$. Its auto-correlation during the service life of $[t_0, t_T]$ is described as $\rho_l(\tau)$, where τ is a time interval. $\rho_l(\tau) = 0$ means that the random variables included in the stochastic process are independent during the service cycle. Thus, a random variable can be treated as a special case of stochastic process.

The performance reliability evolves into the probability that the stress balance in the IGBT meets the requirements during the service cycle. The time-variant reliability is formulated as:

$$R^T = \Pr\left(g\left(\boldsymbol{X}, \boldsymbol{P}(t), t\right) \geq 0\right), \quad \forall t \in [t_0, t_T] \tag{2}$$

Also, the time-variant reliability can be described by a reliability index β^T. The relationship between the two is written as :

$$R^T = \Phi\left(\beta^T\right), \quad \beta^T = \Phi^{-1}\left(R^T\right) \tag{3}$$

where Φ and Φ^{-1} denote the standard normal cumulative distribution function and its inverse, respectively. Compared with the static uncertain condition, the stress balance of IGBT presents a greater probability of failure during the service cycle, i.e., reliability degradation.

III. TIME-VARIANT RELIABILITY OPTIMIZATION MODELLING FOR STRESS BALANCE

An IGBT design problem with n-number of sub-modules is considered. There are two constraints for the stress balance. ① The maximum chip stress (S_U) should be less than a threshold $\left(S_U^{thr}\right)$ to avoid structural cracking. ② The typical chip stress (S_T) should be greater than a threshold $\left(S_T^{thr}\right)$ to ensure adequate thermal contact. The typical stress means the stress at the chip centre. The objective is to optimize the stress balance, defined as $\mathrm{E}\left(S_T/S_U\right)$. E stands for expectation operator.

In the IGBT, the silver sheets adjust the stress difference between the sub-modules [25]. A softer silver sheet (with lower elastic modulus) can compensate for thermal deformation and improve pressure balance [2]. The shape of a silver sheet is a square sheet, and different deformation resistance can be obtained by changing its side length, namely the equivalent elastic modulus. It is used as a design vector, written as $\boldsymbol{X} = (X_1, X_2, \ldots, X_n)$. For a silver sheet, the relationship between the equivalent elastic modulus (X_i), side length (L_i), and material elastic modulus (E_0) is expressed as:

$$L_i = L_0 \cdot \sqrt{\frac{X_i}{E_0}} \tag{4}$$

where L_0 denotes the chip side length. When the side lengths of a silver sheet and a chip are equal, $X_i = E_0$. When the stress simulation is invoked by the optimization process, the finite element model usually requires re-meshing. It may lead to a convergence barrier. The equivalent of Eq. (4) avoids the re-meshing in the finite element simulations, thereby solving the convergence issue.

During the service cycle of $[t_0, t_T]$, the time-variant chip heat consumption is measured as $\boldsymbol{P}(t) = (P_1(t), P_2(t), \ldots, P_l(t), \ldots, P_n(t))$. The auto-correlation of $P_l(t)$ can be formulated as a function of $\rho(-\tau)$. The stress balance performances are the functions associated with $\boldsymbol{X}$ and $\boldsymbol{P}$, i.e., $S_U(\boldsymbol{X}, \boldsymbol{P}(t))$ and $S_T(\boldsymbol{X}, \boldsymbol{P}(t))$, forming the function of g in Eq. (2). The objective $\mathrm{E}\left(S_T/S_U\right)$ can be rewritten as $\frac{S_T(\boldsymbol{X}, \boldsymbol{\mu_P})}{S_U(\boldsymbol{X}, \boldsymbol{\mu_P})}$. $\boldsymbol{\mu_X}$, $\boldsymbol{\mu_P}$ represent the mean of $\boldsymbol{X}$ and $\boldsymbol{P}$. Thus, the stress balance time-variant reliability optimization model of the press-pack IGBT is formulated as follows:

$$\begin{aligned}
&\max_{\boldsymbol{X}} f = S_T(\boldsymbol{X}, \boldsymbol{\mu_P})/S_U(\boldsymbol{X}, \boldsymbol{\mu_P}) \\
&\text{s.t. } \beta_j^T \geq \beta_j^t, \quad j = 1, 2 \\
&\quad \beta_j^T = \Phi^{-1}\left(\Pr\left(g_j(\boldsymbol{X}, \boldsymbol{P}(t), t) \geq 0\right)\right) \\
&\quad g_1 = S_U^{thr} - S_U(\boldsymbol{X}, \boldsymbol{P}(t), t) \\
&\quad g_2 = S_T(\boldsymbol{X}, \boldsymbol{P}(t), t) - S_T^{thr} \\
&\quad \forall t \in [t_0, t_T], \quad X_i^L \leq X_i \leq X_i^R, \ i = 1, 2, \cdots, n
\end{aligned} \tag{5}$$

where X_i^R and X_i^L are the upper and lower bounds of the design variables, respectively. β_j^t, $j = 1, 2$ represent the target reliability indexes.

The time-variant reliability optimization is essentially nested, as shown in Fig. 3. The outer layer optimizes the design points, and the inner layer analyzes the time-variant reliability at each design point. Even if high-efficiency algorithms (e.g., the quasi-Newton algorithm and sequential quadratic programming) are adopted [30], dozens or hundreds of reliability analyses (Iteration k × Dimensions n) are required. The static reliability analysis is an optimization process that repeatedly invokes the time-consuming simulation of IGBT. Further considering the time-variant reliability analysis of the service cycle, the simulation evaluations (N_F) are dozens of times that of the static analysis. Time for a single finite element simulation (T_F) may take several minutes or hours. The computational cost of IGBT time-variant reliability optimization is calculated as $k \times n \times N_F \times T_F$.

According to a rough estimate, the solution time is 10^5 hours $(10 \times 10 \times 10^3 \times 1)$, i.e., 11.4 years. The solution efficiency cannot meet the needs of engineering applications. Therefore, it is necessary to develop an efficient algorithm according to the features of IGBT time-variant reliability optimization.

IV. FORMULATION OF DECOUPLING ALGORITHM

To address the efficiency issue, a decoupling algorithm is proposed. It decouples the time-variant reliability optimization into a sequential iteration with time-variant reliability analysis and static reliability optimization. The time-variant continuity of stress in the IGBT is utilized to reduce the times of searches for the most likelihood point in the reliability analysis.

A. TIME-VARIANT RELIABILITY ANALYSIS

The improved time-variant progress discretization method is employed to solve the time-variant reliability constraints in Eq. (5) [31]. Firstly, the time-variant reliability analysis is transformed into a system reliability problem by discretizing the stochastic processes and performance functions during the service cycle. Secondly, the static reliability analysis is performed on the period unit, and the correlation coefficient matrices of the performance functions are calculated. Finally, the IGBT time-variant reliability is calculated using the unit reliability analysis results and correlation coefficient matrices.

The service cycle $[t_0,\ t_T]$ is discretized into m-number of equal period units $(t_1, t_2, \ldots, t_i, \ldots, t_m)$. Correspondingly, each time-variant performance function is discretized into m-number of static performance functions. m is the discrete number. t_i represents the i-th unit, i.e., $t_i = (i-0.5)\cdot(t_T - t_0)/m$. The time-variant reliability analysis is converted to the reliability analysis of the series system composed of the units. Thus, $\Pr\left(g_j\left(\boldsymbol{X}, \boldsymbol{P}\left(t\right), t\right) \geq 0\right)$ in Eq. (5) is equivalent to

$$R_j^T = \Pr\left(\bigcap_{i=1}^{m}\left(g_j\left(\boldsymbol{X}, \boldsymbol{P}\left(t_i\right),\ t_i\right) \geq 0\right)\right) \tag{6}$$

where $\boldsymbol{P}\left(t_i\right) = \left(P_1\left(t_i\right), P_2\left(t_i\right), \ldots, P_n\left(t_i\right)\right)$ is the n-dimensional random vector in the unit of t_i after $\boldsymbol{P}\left(t\right)$ is discretized. According to the reliability analysis principle of a series system [32], Eq. (6) can be solved by

$$R_j^T = \Phi_m\left(\beta_j\left(t_1\right), \beta_j\left(t_2\right), \ldots, \beta_j\left(t_m\right), \boldsymbol{\rho}_j\right) \tag{7}$$

where Φ_m is the m-dimensional standard normal distribution function, and multi-dimensional normal distribution calculation refers to the literature [33]. $\beta_j\left(t_i\right)$ represents the reliability index of the performance function of $g_j\left(\boldsymbol{X}, \boldsymbol{P}\left(t_i\right),\ t_i\right)$. $\boldsymbol{\rho}_j$ denotes the correlation coefficient matrix of g_j.

The first-order second-moment method is adopted to calculate $\beta_j\left(t_i\right)$ and g_j [11]. $\boldsymbol{P}^M\left(t_i\right)$ denotes the most likelihood point, with the maximum joint probability density. A linear approximation to g_j at the point can be used to calculate the correlation coefficient matrix [20]. The linear approximation

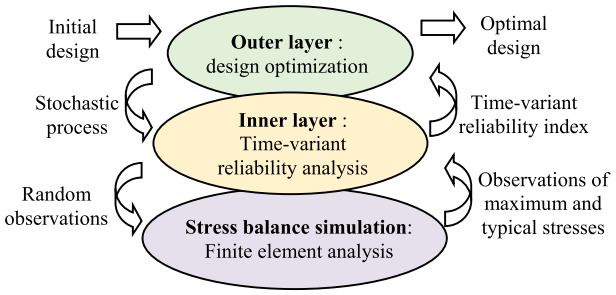

FIGURE 3. The nested optimization in the time-variant reliability optimization.

is derived as

$$L_j = g_j\left(\boldsymbol{X}, \boldsymbol{P}^M\left(t_i\right),\ t_i\right) + \left(\boldsymbol{P}\left(t_i\right) - \boldsymbol{P}^M\left(t_i\right)\right)^{\mathrm{T}} \cdot \nabla g_j\left(\boldsymbol{X}, \boldsymbol{P}^M\left(t_i\right),\ t_i\right) \tag{8}$$

where ∇g_j represents the gradient vector at the point of $\boldsymbol{P}^M\left(t_i\right)$. A component of $\rho_j\left(t_i,\ t_i+\tau\right)$ in $\boldsymbol{\rho}_j$ represents the correlation coefficient between $L_j\left(t_i\right) = L_j\left(\boldsymbol{X}, \boldsymbol{P}\left(t_i\right),\ t_i\right)$ and $L_j\left(t_i+\tau\right) = L_j\left(\boldsymbol{X}, \boldsymbol{P}\left(t_i+\tau\right),\ t_i+\tau\right)$. τ means a time interval. $\rho_j\left(t_i,\ t_i+\tau\right)$ is derived as

$$\begin{aligned}
&\rho_j\left(t_i,\ t_i+\tau\right) \\
&= \frac{\mathrm{COV}\left(L_j\left(t_i\right), L_j\left(t_i+\tau\right)\right)}{\sigma\left(L_j\left(t_i\right)\right)\cdot\sigma\left(L_j\left(t_i+\tau\right)\right)} \\
&= \frac{\sum_{l=1}^{n}\nabla g_{j,\,l}\left(t_i\right)\cdot\nabla g_{j,\,l}\left(t_i+\tau\right)\cdot\rho\left(P_l\left(t_i\right), P_l\left(t_i+\tau\right)\right)}{\sigma\left(L_j\left(t_i\right)\right)\cdot\sigma\left(L_j\left(t_i+\tau\right)\right)}
\end{aligned} \tag{9}$$

where COV indicates a covariance operation. σ denotes a standard deviation operation. $\nabla g_{j,\,l}\left(t_i\right)$ represents the l-th component of $\nabla g_j\left(\boldsymbol{X}, \boldsymbol{P}^M\left(t_i\right),\ t_i\right)$. $\rho\left(P_l\left(t_i\right), P_l\left(t_i+\tau\right)\right)$ represents the auto-correlation function of the stochastic process P_l.

B. THE FLOWCHART OF DECOUPLING ALGORITHM

The time-variant reliability analysis method for the IGBT stress balance is given in the previous section. It is an optimization process embedded with time-consuming simulations. The time-variant reliability optimization requires repeated calls to the reliability analysis, thus involving a nested optimization. To improve efficiency, a decoupling algorithm with the sequential iteration of static reliability optimization and time-variant reliability analysis is proposed.

In the k-th iteration, the time-variant reliability analysis is performed at the previous solution $\boldsymbol{X}^{(k-1)}$. According to the research in Part A, two issues need to be solved: the efficiency of searching for the most likelihood point, and how to determine the discrete number (m). ① The time-variant continuity of the stress response is exploited to reduce the times of searches for the most likelihood points. The stress response varies with time, but its functional form is constant for each period unit. Thus, the most likelihood points are close

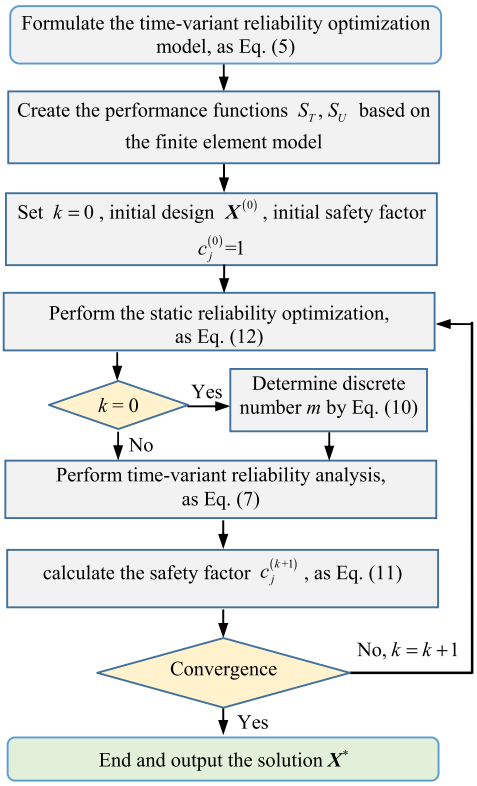

FIGURE 4. The flowchart of the decoupling algorithm.

in the standard normal space [9]. The most likelihood point is searched in the first unit t_1 and extended to other units $t_i = t_2, t_3, \ldots, t_m$. m-number of searches are converted into a single search, so the efficiency is significantly improved. ② A convergence mechanism is developed to determine the discrete number m. A trial-by-trial identification is used to search for m, i.e., starting from $m = 1$ to calculate $R_j^T(m)$ based on Eq. (7) until two-step continuous convergence. The convergence criterion is established as

$$\left|\frac{R_j^T(m) - R_j^T(m-1)}{R_j^T(m)}\right| \le \varepsilon \;\&\; \left|\frac{R_j^T(m) - R_j^T(m-2)}{R_j^T(m)}\right| \le \varepsilon \tag{10}$$

where ε indicates the convergence limit. The value of m obtained in the first iteration applies all iterations.

After solving the above issues, an iterative mechanism for the time-variant reliability optimization is created. A nonlinear equation is formulated according to Eq. (5) and Eq. (7), expressed as:

$$\Phi^{-1}\left(\Phi_m\left(\begin{matrix} c_j^{(k+1)} \cdot \beta_j^{(k)}(t_1), c_j^{(k+1)} \cdot \beta_j^{(k)}(t_2) \\ \ldots, c_j^{(k+1)} \cdot \beta_j^{(k)}(t_m), \boldsymbol{\rho}_j \end{matrix}\right)\right) = \beta_j^t \tag{11}$$

where $c_j^{(k+1)}$ represents the safety factor for the j-th constraint at the $k+1$-th iteration. $\beta_j^{(k)}(t_i)$ denotes the static reliability index on the t_i unit at the k-th iteration. Eq. (11) is a root-finding problem for the nonlinear equation, which can be solved by the Newton iterative algorithm [34].

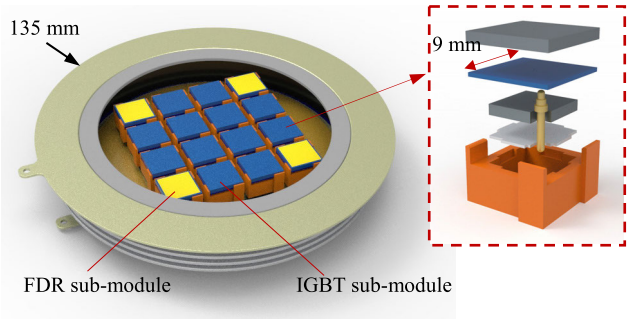

FIGURE 5. The structural diagram of the press-pack IGBT.

TABLE 2. Distribution characteristics of the heat dissipation stochastic proces.

Sub-module	Mean (μ_P)	Standard deviation (σ_P)	Autocorrelation function
IGBT	120W	12W	$\rho = 0.2\exp(-\tau)$
FRD	72W	7.2W	$\rho = 0.2\exp(-0.4\tau)$

The time-variant reliability optimization as Eq. (5) is converged into a static reliability optimization, formulated as:

$$\begin{aligned} &\max_{\boldsymbol{X}} f = S_T(\boldsymbol{X}, \boldsymbol{\mu_P}) / S_U(\boldsymbol{X}, \boldsymbol{\mu_P}) \\ &\text{s.t. } \beta_j^{(k)}(t_1) \ge c_j^{(k)} \cdot \beta_j^t, \quad j = 1, 2 \\ &\quad \beta_j^{(k)} = \Phi^{-1}\left(\Pr\left(g_j(\boldsymbol{X}, \boldsymbol{P}(t_1), t_1) \ge 0\right)\right) \\ &\quad g_1 = S_U^{thr} - S_U(\boldsymbol{X}, \boldsymbol{P}(t_1), t_1) \\ &\quad g_2 = S_T(\boldsymbol{X}, \boldsymbol{P}(t_1), t_1) - S_T^{thr} \\ &\quad X_i^L \le X_i \le X_i^R, \quad i = 1, 2, \cdots, n \end{aligned} \tag{12}$$

The above formula can be solved by existing methods, such as the incremental shifting vector method [35], thereby obtaining the solution $\boldsymbol{X}^{(k)}$ of the current iteration. The time-variant reliability analysis and reliability optimization are performed alternately until meeting the convergence criteria as follows:

$$\begin{cases} \beta_j^T \ge \beta_j^t, \; j = 1, 2 \\ \left|\dfrac{f^{(k)} - f^{(k-1)}}{f^{(k)}}\right| \le \varepsilon \end{cases} \tag{13}$$

The algorithm flowchart is summarized in Fig. 4. The computational cost of the solution depends on the evaluations of the finite element model. The $\boldsymbol{X}$ and $\boldsymbol{P}$ with the higher dimensions result in more evaluations of the finite element model for design optimization and reliability analysis in each iteration. Moreover, the combination of high-dimensional $\boldsymbol{X}$ and $\boldsymbol{P}$ leads to more iterations. Therefore, the dimension of the optimization model and the complexity of the finite element model are the key to the proposed approach efficiency.

V. ENGINEERING APPLICATION

A press-pack IGBT application, as shown in Fig. 5, was used to verify the performance of the proposed time-variant reliability optimization approach. The IGBT device contained

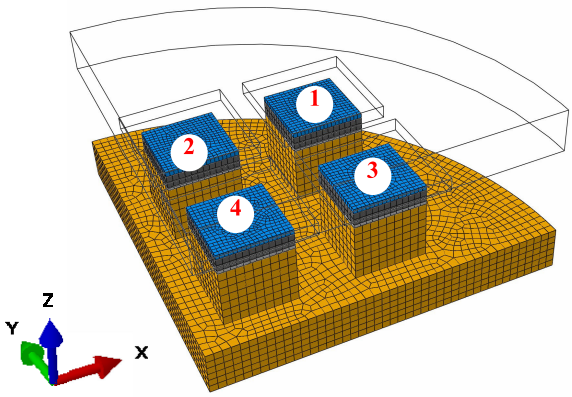

FIGURE 6. The finite element model of the IGBT.

TABLE 3. The material properties of the component.

Properties	Molybdenum	Copper	Silver	Silicon
Elastic Modulus (GPa)	320	77.9	10.5	140
Poisson's Ratio	0.3	0.35	0.31	0.18
Thermal Expansion Coefficient (/K)	5.30E-6	19.0E-6	19.5E-6	2.3E-6
Thermal Conductivity (W/m·K)	126	390	429	703
Specific Heat Capacity (J/kg·K)	250	386	550	20

twelve sub-modules of IGBT and four sub-modules of fast recovery diode. Clamping forces $F = 72$ KN with equal magnitude and opposite directions were applied to the top and bottom surfaces of the IGBT. To dissipate the IGBT heat consumption, the upper and lower surfaces were given liquid cooling conditions. The stress balance performance was defined as an objective function of $f = S_U/S_T$. The reliability indexes of the constraints $g_1 = S_U^{thr} - S_U \geq 0$ and $g_2 = S_T - S_T^{thr} \geq 0$ should be greater than $\beta_j^t = 2.5,\ j = 1, 2$, where $S_U^{thr} = 78$ MPa and $S_U^{thr} = 5$ MPa. The service cycle of IGBT was 24 hours, i.e., $\forall t \in [0,\ 24]$. The design vector $\boldsymbol{E}$ consisted of the equivalent elastic modulus of the silver sheet in the sub-modules. The time-variant uncertain parameters were the chip heat consumption, described as the stochastic processes in Table 2.

A. STRESS SIMULATION AND EXPERIMENT

The first step in the time-variant reliability optimization was to create a finite element model of the IGBT to analyze the stress balance performance, i.e., the maximum stress (S_U) and typical stresses (S_T) of the chips. The commercial finite element software of ABAQUS/CAE (Version 6.13) was employed. Considering the symmetry of the structure, boundary conditions and loads, a 1/4-type finite element model was established, as shown in Fig. 6. The model ignored the contact pins because their diameter is much smaller than the sub-module side length and had little influence on the stress

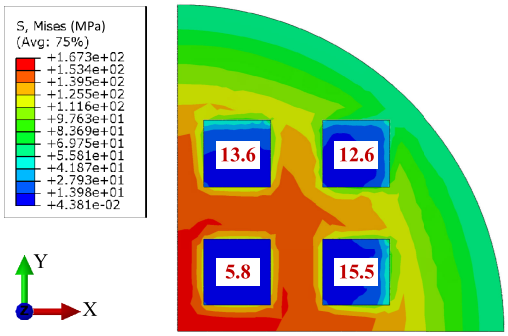

FIGURE 7. The stress distribution on the chips.

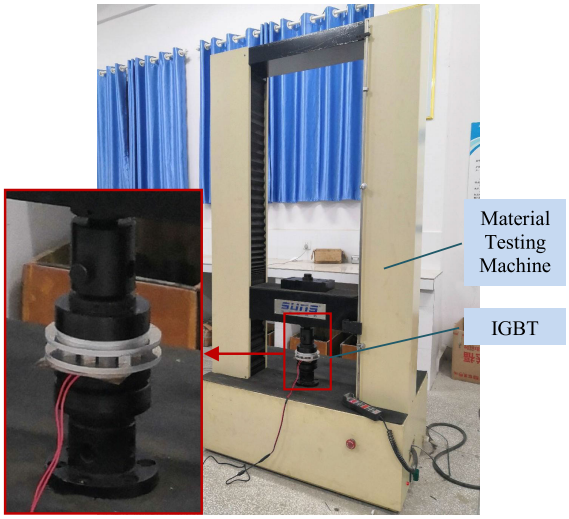

FIGURE 8. The pressure distribution test bench.

distribution. The IGBT sub-modules are marked as white numbers ①∼③, and the sub-module of the fast recovery diode is marked as ④. The internal structure of the sub-modules is shown in Fig. 1. Table 3 lists the mechanical and thermal properties of the IGBT components.

According to the IGBT operating conditions, the loads and boundary conditions in the finite element model were set as follows: A fixed constraint is placed on the emitter lower surface. A uniform force $F = 12$ kN is applied on the collector upper surface. Heat exchange conditions were established on the surfaces to simulate the liquid cooling effect, i.e., the sink temperature of 35 °C and the heat transfer coefficient of 0.01 W/mm^2. The contact behaviour between the components was characterized by pressure-dependent thermal resistance and normal hard contact [36]. The initial values of the design variables are $X_i = E_0,\ i = 1, 2, 3, 4$, where $E_0 = 10.5$ GPa represents the elastic modulus of silver. It means that the side lengths of the silver sheets and chips are equal, i.e., $L_i = L_0 = 9$ mm, $i = 1, 2, 3, 4$. The chip heat consumption was defined as the mean values of the random processes in Table 2, i.e., $\mu_{P_i} = 120$ W, $i = 1, 2, 3$ and $\mu_{P_4} = 72$ W. The finite element model contains 18 elements and 28,624 eight-node thermally coupled hexahedral elements. Using a conventional computer (e.g., CPU_i7, RAM_8g) to solve it, a single simulation took about ten minutes. The stress simulation results

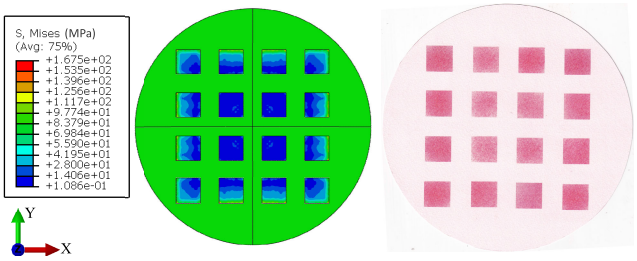

FIGURE 9. The numerical and experimental results of the pressure distribution.

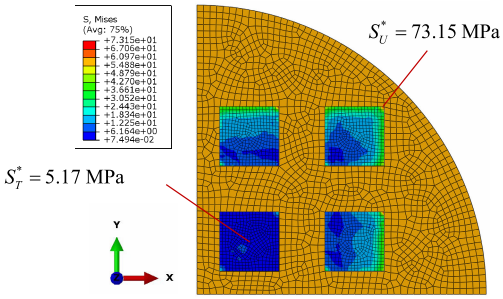

FIGURE 10. The stress distribution at optimal design.

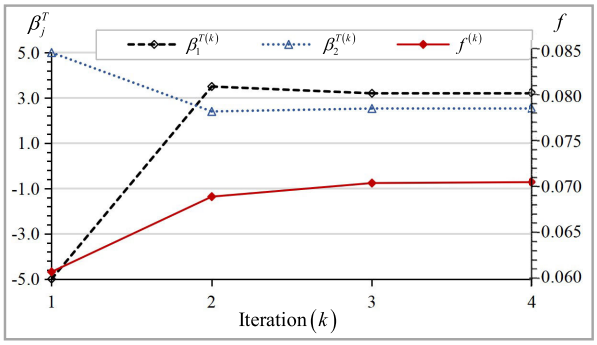

FIGURE 11. The iterations of the objective value and reliability indexes.

are shown in Fig. 7, marking the Von-Mises stress at the centre of each chip. The stress distribution presents a significant imbalance. The upper bound (15.5 MPa) and the lower bound (5.8 MPa) appear on Chip_4 and Chip_3, and the former is 2.6 times larger than the latter.

To verify the accuracy of the finite element simulation, a stress distribution experiment was carried out under a coupled mechanical/thermal condition, as shown in Fig. 8. The experimental bench was composed of the material testing machine (Model: CMT5504 by SASTEST) and the studied IGBT. A temperature-controlled heating membrane was pasted on the emitter lower surface to simulate the IGBT heat consumption. The clamping force was provided by the material testing machine. The mechanical and thermal loads were applied in three stages: contacting, heating and clamping. Firstly, a slight clamping force was loaded onto the IGBT to bring the components into contact. Secondly, the heating film was turned on and held for twenty minutes, with the temperature set at 45 °C until thermal equilibrium. Thirdly, the clamping force was increased to 72 kN at the rate of 12 kN/min, and maintained for five minutes.

Due to engineering limitations, the experimental bench was slightly different from the actual IGBT operating conditions. The limitations were in load application and stress measurement. The components are small and in contact, leaving no room for stress sensors and heating membranes. Thus, we replaced the chip self-heating effect with the temperature load. And the FUJI pressure-sensitive film was adopted to measure the pressure distribution, which is an intuitive and commonly used method for pressure distribution measurements [37]. Red spots appear on the film where pressure is loaded, and the colour density changes with the pressure level. The films are divided into several pressure levels according to the measurement ranges, and we choose the film with the pressure range of [2.5 MPa, 10 MPa].

The experimental results are shown in Fig. 9. It can be seen that the pressure distribution in the IGBT was not uniform under the coupled mechanical/thermal condition. The colour density at the border was higher than that at the middle, i.e., the sub-modules at the border were subject to the higher stresses. The conditions of the simulation model were adjusted to be consistent with the experiment, i.e., using the temperature load to simulate the chip power consumption. The experimental results were generally consistent with the simulation results. Besides, the simulation modeling in this study referred to the literature [36], which revealed the influence of temperature on the pressure distribution of the IGBT with 44 sub-modules. The accuracy of the simulation model was verified by the experimental results. Therefore, the experiments in this study and existing literature support that the simulation model can predict the IGBT stress distribution, providing effective performance functions for the time-variant reliability optimization.

B. OPTIMIZATION MODELLING AND SOLUTION

For the IGBT device with sixteen sub-modules, a time-variant reliability optimization model was established as:

$$\begin{aligned}
&\min_{\boldsymbol{X}} f = S_U\left(\boldsymbol{X},\ \boldsymbol{\mu_P}\right)/S_T\left(\boldsymbol{X},\ \boldsymbol{\mu_P}\right)\\
&\text{s.t. } \beta_j^T \geq \beta_j^t = 2.5, \quad j = 1, 2\\
&\quad \beta_j^T = \Phi^{-1}\left(\Pr\left(g_j\left(\boldsymbol{X}, \boldsymbol{P}\left(t\right), t\right) \geq 0\right)\right)\\
&\quad g_1 = S_U^{thr} - S_U\left(\boldsymbol{X}, \boldsymbol{P}\left(t\right), t\right),\ S_U^{thr} = 78 \text{ MPa}\\
&\quad g_2 = S_T\left(\boldsymbol{X}, \boldsymbol{P}\left(t\right), t\right) - S_T^{thr},\ S_T^{thr} = 5 \text{ MPa}\\
&\quad \forall t \in [0,\ 24], \quad X_i^L \leq X_i \leq X_i^R,\ i = 1, 2, 3, 4
\end{aligned} \tag{14}$$

The numerical analysis software of MATLAB (Version R2013b) was adopted in the engineering application. $X_i^0 = E_0,\ i = 1, 2, 3, 4$ was selected as the initial design point. At this point, the maximum stress was $S_U^{(0)} = 89.45$ MPa, the typical stress was $S_T^{(0)} = 5.44$ MPa, and the objective value was $f^{(0)} = 0.0608$. The time-variant reliability indexes of the two constraints were $\left(\beta_1^{T(0)},\ \beta_2^{T(0)}\right) = (< -5,\ > 5)$. The first constraint was not satisfied, while the second was over-satisfied. The decoupling algorithm was applied to solve

TABLE 4. The results of time-variant reliability optimization.

Results	Pre-optimization	Post-optimization	Comparison
f	0.0608	0.0707	Improved by 16.3%
$\beta_1^T, \beta_1(t_1)$	-5, -5	3.22, 3.45	From unsatisfied to satisfied
$\beta_2^T, \beta_2(t_1)$	5, 5	2.54, 2.89	From over satisfied to just satisfied

Eq. (14), and the optimal solution was obtained after four iterations, i.e., $X_i^* = (6744, 2538, 7469, 2656)$ MPa. As shown in Fig. 10, the maximum stress was $S_U^* = 73.15$ MPa, the typical stress was $S_T^* = 5.17$ MPa, and the objective value is $f^* = 0.0707$ at the optimal solution. The static reliability indexes of the constraints (i.e., the reliability indexes in the t_1 unit) were $\beta_1^*(t_1) = 2.89$. Considering the service cycle, the time-variant reliability indexes of two constraints were $\beta_1^{T*} = 3.22$ and $\beta_2^{T*} = 2.54$, satisfying $\beta_j^{T*} \geq \beta_j^t = 2.5,\ j = 1, 2$. The iterative process of the objective value $\left(f^{(k)}\right)$ and reliability indexes $\left(\beta_1^{T(k)},\ \beta_2^{T(k)}\right)$ is shown in Fig. 11. The solution called the finite element simulation 316 times and took 53 hours.

The optimal solution $(\boldsymbol{X}^*)$ of the equivalent elastic modulus was converted into the side length $\boldsymbol{L}^* = (7.2,\ 4.4,\ 7.6,\ 4.5)$ mm of the silver sheet by Eq. (4). The finite element model described above is modified to obtain the maximum and typical stresses of $(73.41,\ 5.14)$ MPa at the optimal side length. The results were close to $\left(S_U^*,\ S_T^*\right) = (73.15,\ 5.17)$ MPa, with errors of 0.36% and 0.39%. It verified the validity of the conversion between the equivalent elastic modulus and the structural size.

C. DISCUSSION OF RESULTS

The stress balance performance comparison before and after the IGBT time-variant reliability optimization is listed in Table 4. After optimization, the stress balance performance is improved from $f^{(0)} = 0.0608$ to $f^* = 0.0707$, increasing by 16.3%. At the optimal solution, the static and time-variant reliability indexes of the first constraint are 3.45 and 3.22, and those of the second constraint are 2.89 and 2.54. As analyzed before, the time-variant uncertainty leads to the degradation of IGBT stress balance reliability during the service cycle. Therefore, to obtain a reliable solution, the IGBT reliability degradation during the service period must be considered. The solution of the proposed approach satisfies two time-variant reliability constraints and is feasible. The first constraint changes from unsatisfied to satisfied, and the second changes from over-satisfied to just-satisfied. It suggests that the proposed approach can solve the time-variant reliability design problem of the press-pack IGBT.

To investigate the efficiency and accuracy of the proposed approach, it was compared with a conventional double-loop approach [38]. The Double-loop approach means that the outer layer optimizes the design point by the sequential quadratic programming [30], and the inner layer performs the time-variant reliability analysis. The double-loop approach has high precision and is usually employed to obtain a reference solution, but its computational cost is high [39]. Unfortunately, the double loop approach with invoking the finite element model was not feasible in efficiency. To make the double-loop approach viable in this comparative study, second-order polynomial response surfaces were established for the finite element model. With one hundred random samples, the approximate analytical expressions of the performance functions were formulated as:

$$\begin{aligned} S_U &= 58.6 + 10^{-3} \cdot (-1.36 \cdot X_1 + 3.76 \cdot X_2 - 0.02 \cdot X_3 \\ &\quad + 2.53 \cdot X_4) \\ &\quad + 10^{-7} \cdot (0.58 \cdot X_1^2 - 1.76 \cdot X_2^2 - 3.09 \cdot X_4^2) + 10^{-2} \\ &\quad \cdot (10.5 \cdot P_2 - 6.01 \cdot P_4) + 10^{-7} \times (4.86 \cdot X_1 \cdot P_1 \\ &\quad - 12.21 \cdot X_2 \cdot P_2) \\ &\quad + 10^{-7} \cdot (-1.75 \cdot X_3 \cdot P_3 + 10.46 \cdot X_4 \cdot P_4) \\ S_T &= 3.48 + 10^{-4} \cdot (1.18 \cdot X_1 - 0.28 \cdot X_2 + 0.16 \\ &\quad \cdot X_3 - 3.85 \cdot X_4) \\ &\quad + 10^{-8} \cdot (-0.44 \cdot X_1^2 + 5.55 \cdot X_4^2) + 10^{-3} \\ &\quad \cdot (8.46 \cdot P_2 + 1.19 \cdot P_4) + 10^{-7} \cdot (-2.68 \cdot X_1 \\ &\quad \cdot P_1 + 2.75 \cdot X_2 \cdot P_2) \\ &\quad + 10^{-7} \cdot (9.86 \cdot X_3 \cdot P_3 + 5.78 \cdot X_4 \cdot P_4) \end{aligned} \tag{15}$$

TABLE 5. The comparison of the proposed and double-loop approaches.

Results	Proposed approach	Double-loop approach	Difference
$\boldsymbol{X}^*$ (MPa)	6964, 2496, 7011, 2493	6429, 2456, 7101, 2533	5.3%
f^*	0.0735	0.0732	0.4%
Function evaluations	304	101,632	334 times
Computational time (hours)	50.7	16939	334 times

For objective comparison, the proposed approach was applied again for the time-variant reliability optimization using Eq. (15) as the performance functions. Although the response surface was used in the comparative study, we suggest that the reliability optimization in practice should directly invoke the finite element model to avoid the errors introduced by the response surfaces. Thus, the time consumption of the finite element analysis was included in the computational cost.

The numerical results of the two approaches are listed in Table 5. Regarding efficiency, the proposed approach called the performance function 304 times, and the computational time was 50.7 hours. The functional evaluations were 101,632 times, and the computational time was

16,939 hours (1.93 years). The efficiency advantage of the proposed approach is significant, satisfying engineering requirements. In accuracy, the objective value of the proposed approach is close to the reference solution, with a difference of 0.4%. It demonstrates the approach's accuracy.

VI. CONCLUSION

The stress imbalance in the press-pack IGBT seriously affects the thermal and electrical contacts between the components, resulting in its performance degradation. The effects of stress imbalances are exacerbated by time-variant uncertain loads and conditions. In this paper, a time-variant reliability optimization approach is proposed to address the reliability optimization modelling and solution for the press-pack IGBT involving stochastic processes. The contributions of this study are summarized below. Firstly, the performance functions of the maximum and typical stresses in the IGBT chips are established for the objective and constraints. And a time-variant reliability optimization model of IGBT is formulated considering the reliability degradation of stress balance. Secondly, a decoupling algorithm is proposed, separating the time-variant reliability analysis from the design optimization. The nested optimization is decoupled into a sequential iteration with static reliability optimization and time-variant reliability analysis, significantly reducing the reliability analysis evaluations. Thirdly, an approximation strategy is given to reduce the searches for the most likelihood point by utilizing the time-variant continuity of the stress response. It significantly improves the efficiency of time-variant reliability analysis. The numerical and experimental results on the actual IGBT demonstrate the accuracy of the stress simulation. On this basis, the time-variant reliability optimization improves the stress balance performance by 16.3%, and the reliability indexes meet the constraints. Taking the double-loop approach as a benchmark, the difference between the solution of the proposed approach and the reference solution is 0.4%, and the efficiency is 334 times that of the double-loop approach. The performance advantages in accuracy and efficiency support the excellent potential of the approach in engineering applications. In the future, we will explore experimental strategies to validate the proposed approach in an offshore wind power system and advanced time-variant reliability optimization approaches for power semiconductor devices involving high-dimensional stochastic processes.

REFERENCES

[1] F. Niedernostheide, H. Schulze, T. Laska, and A. Philippou, "Progress in IGBT development," *IET Power Electron.*, vol. 11, no. 4, pp. 646–653, Feb. 2018, doi: 10.1049/iet-pel.2017.0499.

[2] E. Deng, Z. Zhao, Q. Xin, J. Zhang, and Y. Huang, "Analysis on the difference of the characteristic between high power IGBT modules and press pack IGBTs," *Microelectron. Rel.*, vol. 78, pp. 25–37, Nov. 2017, doi: 10.1016/j.microrel.2017.07.095.

[3] S. Dai, Z. Wang, H. Wu, X. Song, G. Li, and V. Pickert, "Thermal and mechanical analyses of clamping area on the performance of press-pack IGBT in series-connection stack application," *IEEE Trans. Compon., Packag. Manuf. Technol.*, vol. 11, no. 2, pp. 200–211, Feb. 2021, doi: 10.1109/TCPMT.2021.3052175.

[4] T. Poller, T. Basler, M. Hernes, S. D'Arco, and J. Lutz, "Mechanical analysis of press-pack IGBTs," *Microelectron. Rel.*, vol. 52, nos. 9–10, pp. 2397–2402, Sep. 2012, doi: 10.1016/j.microrel.2012.06.079.

[5] A. A. Hasmasan, C. Busca, R. Teodorescu, L. Helle, and F. Blaabjerg, "Electro-thermo-mechanical analysis of high-power press-pack insulated gate bipolar transistors under various mechanical clamping conditions," *IEEJ J. Ind. Appl.*, vol. 3, no. 3, pp. 192–197, 2014, doi: 10.1541/ieejjia.3.192.

[6] L. Zhou, S. Zhou, and M. Xu, "Investigation of gate voltage oscillations in an IGBT module after partial bond wires lift-off," *Microelectron. Rel.*, vol. 53, no. 2, pp. 282–287, Feb. 2013, doi: 10.1016/j.microrel.2012.08.024.

[7] W. Tian, W. Chen, B. Ni, and C. Jiang, "A single-loop method for reliability-based design optimization with interval distribution parameters," *Comput. Methods Appl. Mech. Eng.*, vol. 391, Mar. 2022, Art. no. 114372, doi: 10.1016/j.cma.2021.114372.

[8] A. Bajrić, J. Høgsberg, and F. Rüdinger, "Evaluation of damping estimates by automated operational modal analysis for offshore wind turbine tower vibrations," *Renew. Energy*, vol. 116, pp. 153–163, Feb. 2018, doi: 10.1016/j.renene.2017.03.043.

[9] Z. L. Huang, C. Jiang, X. M. Li, X. P. Wei, T. Fang, and X. Han, "A single-loop approach for time-variant reliability-based design optimization," *IEEE Trans. Rel.*, vol. 66, no. 3, pp. 651–661, Sep. 2017, doi: 10.1109/TR.2017.2703593.

[10] B. Liu, F. Xiao, Y. Luo, Y. Huang, and Y. Xiong, "A multi-timescale prediction model of IGBT junction temperature," *IEEE J. Emerg. Sel. Topics Power Electron.*, vol. 7, no. 3, pp. 1593–1603, Sep. 2019, doi: 10.1109/JESTPE.2018.2888506.

[11] R. H. Lopez and A. T. Beck, "Reliability-based design optimization strategies based on FORM: A review," *J. Brazilian Soc. Mech. Sci. Eng.*, vol. 34, no. 4, pp. 506–514, Dec. 2012, doi: 10.1590/S1678-58782012000400012.

[12] S. Missoum, C. Dribusch, and P. Beran, "Reliability-based design optimization of nonlinear aeroelasticity problems," *J. Aircr.*, vol. 47, no. 3, pp. 992–998, May 2010, doi: 10.2514/1.46665.

[13] X. Xu, X. Chen, Z. Liu, J. Yang, Y. Xu, Y. Zhang, and Y. Gao, "Multi-objective reliability-based design optimization for the reducer housing of electric vehicles," *Eng. Optim.*, vol. 54, no. 8, pp. 1324–1340, May 2021, doi: 10.1080/0305215X.2021.1923704.

[14] A. Namdari and Z. S. Li, "An entropy-based approach for modeling lithium-ion battery capacity fade," in *Proc. RAMS*, Palm Springs, CA, USA, 2020, pp. 1–7, doi: 10.1109/RAMS48030.2020.9153698.

[15] A. Namdari and Z. S. Li, "A multiscale entropy-based long short term memory model for lithium-ion battery prognostics," in *Proc. IEEE ICPHM*, Detroit, MI, USA, Jun. 2021, pp. 1–6, doi: 10.1109/ICPHM51084.2021.9486674.

[16] E. Gatta, J. Mairesse, L. Deruyter, J. Marrocco, G. Van Camp, H. Bouwalerh, J.-M. Lo Guidice, S. Morley-Fletcher, F. Nicoletti, and S. Maccari, "Reduced maternal behavior caused by gestational stress is predictive of life span changes in risk-taking behavior and gene expression due to altering of the stress/anti-stress balance," *NeuroToxicology*, vol. 66, pp. 138–149, May 2018, doi: 10.1016/j.neuro.2018.04.005.

[17] Y. Liu, N. Lu, and X. Yin, "A hybrid method for structural system reliability-based design optimization and its application to trusses," *Qual. Rel. Eng. Int.*, vol. 32, no. 2, pp. 595–608, Feb. 2015, doi: 10.1002/qre.1775.

[18] M. Xiong and Y. Huang, "A review of time-dependent reliability analyses of slopes: Research progress, influencing factors, and future research directions," *Transp. Geotechnics*, vol. 37, Nov. 2022, Art. no. 100867, doi: 10.1016/j.trgeo.2022.100867.

[19] A. Namdari and Z. S. Li, "A review of entropy measures for uncertainty quantification of stochastic processes," *Adv. Mech. Eng.*, vol. 11, no. 6, Jun. 2019, Art. no. 168781401985735, doi: 10.1177/1687814019857350.

[20] C. Jiang, T. Fang, Z. X. Wang, X. P. Wei, and Z. L. Huang, "A general solution framework for time-variant reliability based design optimization," *Comput. Methods Appl. Mech. Eng.*, vol. 323, pp. 330–352, Aug. 2017, doi: 10.1016/j.cma.2017.04.029.

[21] S. Yu, Z. Wang, and D. Meng, "Time-variant reliability assessment for multiple failure modes and temporal parameters," *Struct. Multidisciplinary Optim.*, vol. 58, no. 4, pp. 1705–1717, May 2018, doi: 10.1007/s00158-018-1993-4.

[22] X. Li, G. Chen, Y. Wang, and D. Yang, "A unified approach for time-invariant and time-variant reliability-based design optimization with multiple most probable points," *Mech. Syst. Signal Process.*, vol. 177, Sep. 2022, Art. no. 109176, doi: 10.1016/j.ymssp.2022.109176.

[23] Z. Wu, Z. Chen, G. Chen, X. Li, C. Jiang, X. Gan, H. Qiu, and L. Gao, "An efficient time-variant reliability-based design optimization method based on probabilistic feasible region," *J. Mech. Sci. Technol.*, vol. 37, no. 3, pp. 1375–1387, Feb. 2023, doi: 10.1007/s12206-023-0224-0.
[24] H. Li, R. Yao, W. Lai, H. Ren, and J. Li, "Modeling and analysis on overall fatigue failure evolution of press-pack IGBT device," *IEEE Trans. Electron Devices*, vol. 66, no. 3, pp. 1435–1443, Mar. 2019, doi: 10.1109/TED.2019.2893455.
[25] Z. L. Huang, T. G. Yang, C. B. Li, J. Zheng, and W. X. He, "Optimization of the pressure distribution in press-pack insulated gate bipolar transistors," *Struct. Multidisciplinary Optim.*, vol. 63, no. 2, pp. 855–865, Feb. 2021, doi: 10.1007/s00158-020-02713-1.
[26] Y. L. Xu and J. Chen, "Characterizing nonstationary wind speed using empirical mode decomposition," *J. Struct. Eng.*, vol. 130, no. 6, pp. 912–920, 2004, doi: 10.1061/(ASCE)0733-9445(2004)130:6(912).
[27] B. Fu, J. Zhao, B. Li, J. Yao, A. R. M. Teifouet, L. Sun, and Z. Wang, "Fatigue reliability analysis of wind turbine tower under random wind load," *Struct. Saf.*, vol. 87, Nov. 2020, Art. no. 101982, doi: 10.1016/j.strusafe.2020.101982.
[28] S. V. Dhople, Y. C. Chen, L. DeVille, and A. D. Domínguez-García, "Analysis of power system dynamics subject to stochastic power injections," *IEEE Trans. Circuits Syst. I, Reg. Papers*, vol. 60, no. 12, pp. 3341–3353, Dec. 2013, doi: 10.1109/TCSI.2013.2265972.
[29] F. M. Mele, R. Zárate-Miñano, and F. Milano, "Modeling load stochastic jumps for power systems dynamic analysis," *IEEE Trans. Power Syst.*, vol. 34, no. 6, pp. 5087–5090, Nov. 2019, doi: 10.1109/TPWRS.2019.2940416.
[30] M. A. Valdebenito and G. I. Schuëller, "A survey on approaches for reliability-based optimization," *Struct. Multidisciplinary Optim.*, vol. 42, no. 5, pp. 645–663, Nov. 2010, doi: 10.1007/s00158-010-0518-6.
[31] C. Jiang, X. P. Wei, B. Wu, and Z. L. Huang, "An improved TRPD method for time-variant reliability analysis," *Struct. Multidisciplinary Optim.*, vol. 58, no. 5, pp. 1935–1946, Nov. 2018, doi: 10.1007/s00158-018-2002-7.
[32] M. Ram, "On system reliability approaches: A brief survey," *Int. J. Syst. Assurance Eng. Manage.*, vol. 4, no. 2, pp. 101–117, Jun. 2013, doi: 10.1007/s13198-013-0165-6.
[33] A. Genz, "Numerical computation of multivariate normal probabilities," *J. Comput. Graph. Statist.*, vol. 1, no. 2, pp. 141–149, Jun. 1992, doi: 10.1080/10618600.1992.10477010.
[34] L. Xu, L. Chen, and W. Xiong, "Parameter estimation and controller design for dynamic systems from the step responses based on the Newton iteration," *Nonlinear Dyn.*, vol. 79, no. 3, pp. 2155–2163, Feb. 2015, doi: 10.1007/s11071-014-1801-7.
[35] Z. L. Huang, C. Jiang, Y. S. Zhou, Z. Luo, and Z. Zhang, "An incremental shifting vector approach for reliability-based design optimization," *Struct. Multidisciplinary Optim.*, vol. 53, no. 3, pp. 523–543, Mar. 2016, doi: 10.1007/s00158-015-1352-7.
[36] E. Deng, Z. Zhao, Z. Lin, R. Han, and Y. Huang, "Influence of temperature on the pressure distribution within press pack IGBTs," *IEEE Trans. Power Electron.*, vol. 33, no. 7, pp. 6048–6059, Jul. 2018, doi: 10.1109/TPEL.2017.2749521.
[37] S. Kim and C. Miller, "Validation of a finite element humeroradial joint model of contact pressure using Fuji pressure sensitive film," *J. Biomech. Eng.*, vol. 31, no. 57, pp. 241–262, 2016, doi: 10.2139/ssrn.163156.
[38] X. Zhang, Z. Lu, and K. Cheng, "Reliability index function approximation based on adaptive double-loop Kriging for reliability-based design optimization," *Rel. Eng. Syst. Saf.*, vol. 216, Dec. 2021, Art. no. 108020, doi: 10.1016/j.ress.2021.108020.
[39] M. Li and Z. Wang, "Surrogate model uncertainty quantification for reliability-based design optimization," *Rel. Eng. Syst. Saf.*, vol. 192, Dec. 2019, Art. no. 106432, doi: 10.1016/j.ress.2019.03.039.

HANGYANG LI received the Ph.D. degree from Hunan University, China, in 2020. He is currently with the School of Mechanical and Electrical Engineering, Hunan City University. His research interests include multiphysics coupling analysis and reliability-based design optimization for mechatronics systems

TONGGUANG YANG received the Ph.D. degree from Central South University, China, in 2013. He is currently a Professor with the School of Mechanical and Electrical Engineering, Hunan City University. His current research interests include the grid-connected inverters control for new energy and fault diagnosis for induction motors.

XINGLIN LIU (Graduate Student Member, IEEE) is currently a Research Assistant with the Hunan Provincial Key Laboratory of Energy Monitoring and Edge Computing for Smart City, Hunan City University. Her research interest includes power semiconductor applications.

JINGYI ZHONG is currently a Research Assistant with the Hunan Provincial Key Laboratory of Energy Monitoring and Edge Computing for Smart City, Hunan City University. Her research interest includes application characteristics of IGBT modules.

JIAXIN MO (Graduate Student Member, IEEE) is currently a Research Assistant with the Hunan Provincial Key Laboratory of Energy Monitoring and Edge Computing for Smart City, Hunan City University. Her research interest includes reliability evaluation for electronics.

HAN ZHOU is currently a Research Assistant with the Hunan Provincial Key Laboratory of Energy Monitoring and Edge Computing for Smart City, Hunan City University. His research interests include engineering failure analysis and manufacturing process reliability.

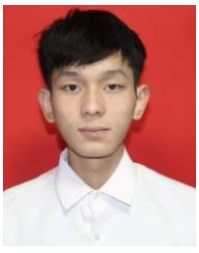

ZHONGKUN XIAO (Graduate Student Member, IEEE) is currently a Research Assistant with the Hunan Provincial Key Laboratory of Energy Monitoring and Edge Computing for Smart City, Hunan City University. His research interests include multiphysics analysis and reliability optimization.